Meteoritics & Planetary Science 37, 565–576 (2002)
Available online at http://www.uark.edu/meteor

Strontium and neodymium isotopic study of Libyan Desert Glass: Inherited Pan-African age signatures and new evidence for target material

PETER SCHAAF[1]* AND DIETER MÜLLER-SOHNIUS[2]

[1]Instituto de Geofísica, Universidad Nacional Autónoma de México, 04510 México, D. F., Mexico
[2]Institut für Mineralogie, Petrologie und Geochemie, Universität München, Theresienstrasse 41, D-80333 München, Germany
*Correspondence author's e-mail address: pschaaf@tonatiuh.igeofcu.unam.mx

(Received 2001 May 2; accepted in revised form 2002 January 4)

Abstract–Libyan Desert Glass (LDG) is an impact-related, natural glass of still unknown target material. We have determined Rb-Sr and Sm-Nd isotopic ratios from seven LDG samples and five associated sandstones from the LDG strewn field in the Great Sand Sea, western Egypt. Planar deformation features were recently detected in quartz from these sandstones. ^{87}Sr/^{86}Sr ratios and ϵ-Nd values for LDG range between 0.71219 and 0.71344, and between –16.6 and –17.8, respectively, and hence are distinct from the less radiogenic ^{87}Sr/^{86}Sr ratios of 0.70910–0.71053 and ϵ-Nd values from –6.9 to –9.6 for the local sandstones from the LDG strewn field. Previously published isotopic ratios from the Libyan BP and Oasis crater sandstones are generally incompatible with our LDG values. LDG formation undoubtedly occurred at 29 Ma, but neither the Rb-Sr nor the Sm-Nd isotopic system were rehomogenised during the impact event, as we can deduce from Pan-African ages of ~540 Ma determined from the regression lines from a total of 14 LDG samples from this work and the literature. Together with similar Sr and Nd isotopic values for LDG and granitoid rocks from northeast Africa west of the Nile, these findings point to a sandy matrix target material for the LDG derived from a Precambrian crystalline basement, ruling out the Cretaceous sandstones of the former "Nubian Group" as possible precursors for LDG.

INTRODUCTION

Libyan Desert Glass (LDG) is a light yellow, sometimes greenish silica glass made up of ~98% SiO_2. It is irregularly distributed in an area of 3500 to 6500 km^2 (Weeks *et al.*, 1984; Murali *et al.*, 1997, respectively) between the nearly north-south trending dunes of the Great Sand Sea in western Egypt (Fig. 1). The estimated quantity of exposed LDG exceeds 1400 tons (Weeks *et al.*, 1984), with fragments ranging from sand-sized grains to pieces heavier than 25 kg (Barrat *et al.*, 1997). An impact origin of LDG is now largely accepted based largely on the presence of baddeleyite (Kleinmann, 1969) and lechatelierite (Storzer and Koeberl, 1991), a local enrichment in meteoritic elements (Koeberl, 2000), and the scarcity of volatiles (Rocchia *et al.*, 1997) in the glass.

For more than three decades attempts to date LDG by means of the K-Ar method have been unsuccessful due to analytical and methodological problems (Müller-Sohnius *et al.*, 1993; Horn *et al.*, 1997). Temperatures in excess of 2200 °C are necessary to quantitatively extract Ar from the samples. The atmospheric portion of the argon has a ^{40}Ar/^{36}Ar ratio of 287.1 ± 1.1, significantly lower than the accepted ^{40}Ar/^{36}Ar value of 295.5 and indicative of the introduction of mass-fractionated argon into the glass, possibly during the impact event. This phenomenon, together with the presence of inherited Ar in the glass, are the main reasons for not obtaining geologically meaningful ages for the LDG with the K-Ar method.

On the other hand, consistent ages of ~29 Ma have been obtained by the fission-track method for the formation of LDG (Gentner *et al.*, 1969; Bigazzi and de Michele, 1997; Horn *et al.*, 1997). This is generally interpreted as the age of the glass-forming impact event. However, it is still not clear if LDG was formed by the impact of a meteorite (*e.g.*, Rocchia *et al.*, 1997) or a comet (Seebaugh and Strauss, 1984) into a highly siliceous target material.

In the area of the LDG strewn field and surroundings, no impact crater structures have yet been found, and the nearest comparable structures are the BP and Oasis craters in eastern Libya, ~130 to 150 km west of the LDG occurrence (Fig. 1), although no LDG fragments have been found in the area of the Libyan craters. Abate *et al.* (1999) presented some petrographic and geochemical similarities between LDG and BP and Oasis crater rocks, but age determinations of both crater structures have not yet been performed.

The best compilation of multidisciplinary investigations on LDG is given in a proceedings volume (edited by de Michele, 1997) of the "Silica '96 Meeting on Libyan Desert Glass and Related Desert Events", held in Bologna, 1996.

Prelude preprint MS#4540

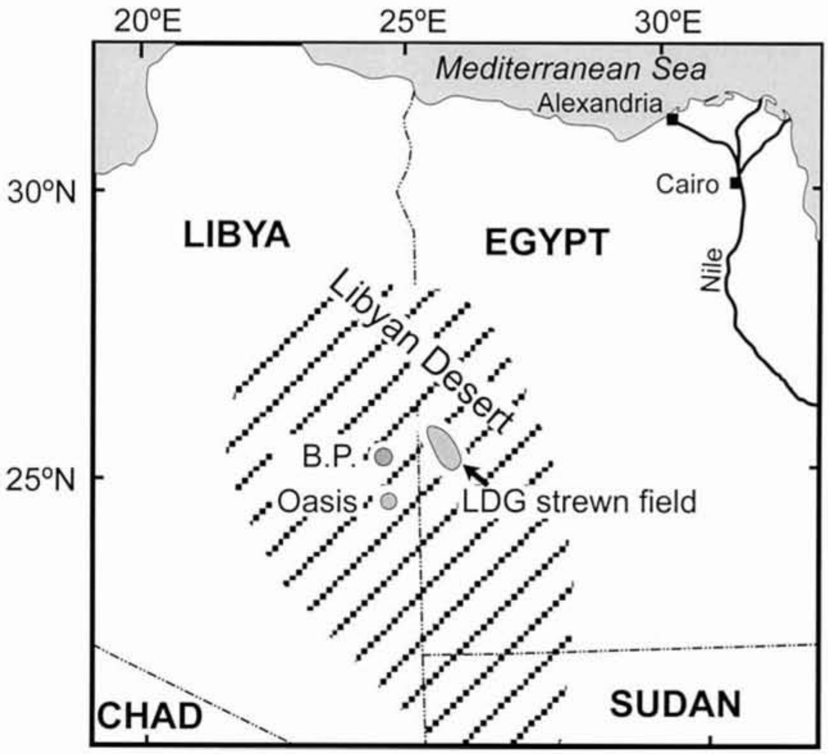

FIG. 1. Sketch map of the Libyan Desert (hatched), showing the locations of the LDG strewn field in western Egypt and the sites of BP and Oasis crater structures in eastern Libya. No LDG samples were found in the area of the Libyan craters.

In this study, we present new Rb-Sr and Sm-Nd isotopic data on seven LDG samples, together with isotopic and geochemical data from five associated sandstones from the LDG strewn field. Our new isotopic database on LDG samples is compared to the sandstone data and data from the literature in order to develop a new model concerning the nature and provenance of LDG target material.

SAMPLES

Seven LDG samples with diameters between 3 and 8 cm were selected, representing the different appearances of the glass: transparent, translucent or milky, sometimes with bubbles and cristobalite spherulites, light yellow and light, intermediate and dark green in colour, with darkish green to nearly black layers or schlieren. Some pieces show signs of wind ablation and etching. A more detailed description of the physical and chemical properties of LDG is given, for instance, by Diemer (1997).

Five sandstones were collected by B. Kleinmann in early 2000 within a very narrow area (25°17.6' N; 25°35.8' E; Kleinmann *et al.*, 2001) in the southern LDG strewn field from outcrops between the north-south striking dunes. They are fine-grained eolian sandstones with quartzitic compositions (quartz with larger, rounded grains and smaller, angular matrix grains) and whitish to yellow colours. The rocks belong to a Cretaceous series often still referred to as "Nubian Sandstone" or parts of the "Nubian Group". Klitzsch (1978) suggested that the term "Nubian Sandstone" should be avoided because it is much too imprecise, characterising different sedimentary units all over southwest Egypt, southeast Libya and adjacent terranes. We have not yet carried out systematic stratigraphic investigations on the sandstone outcrops in the LDG area, but they belong to an upper Cretaceous (probably Coniacian, 88.5–86.6 Ma) sequence called *Saad Formation* (Hermina *et al.*, 1989).

The subsamples investigated in this paper (LDG-S 1–LDG-S 5) are from the same specimens described petrographically by Kleinmann *et al.* (2001). For Sr isotopic investigations it is important to note that matrix carbonates constitute 15% (LDG-S 1), 9% (LDG-S 2), 6.5% (LDG-S 3), 1.5% (LDG-S 4) and 8.5% (LDG-S 5) of the rocks. In two samples (LDG-S 1 and LDG-S 5), Kleinmann *et al.* (2001) have found planar deformation features (PDFs) in quartz grains, which is unequivocal evidence for high-pressure shock metamorphism.

One desert sand sample (LDG-Sd C1) from a LDG collection site was prepared for comparative geochemical analyses.

GEOCHEMISTRY

There have been numerous papers comparing major and trace element data of LDG with sandstone and sand from the region as possible target rock materials (*e.g.*, Weeks *et al.*, 1984; Barrat *et al.*, 1997; Koeberl, 1997; Murali *et al.*, 1997; Abate *et al.*, 1999). One remarkable feature of LDG is its uniformly high SiO_2 content of ~98 wt%. In the residual 2 wt% of the samples, all other major elements are distributed very heterogeneously. Trace element data from different studies are also inconsistent as a result of different methods applied instrumental neutron activation analysis (INAA), inductively coupled plasma-mass spectroscopy (ICP-MS), as well as the heterogeneous physical and chemical properties of LDG. Darkish green samples and especially the dark layers or schlieren show increased Fe, Cr, Co, Ni and platinum group elements, including Ir. Some authors (Murali *et al.*, 1997; Rocchia *et al.*, 1997) have interpreted these enrichments as extraterrestrial components and hence as strong evidence for an impact origin of LDG. These observations were recently confirmed by Os isotope studies (Koeberl, 2000).

Although this work is focused on isotopic investigations, we have determined major element concentrations by x-ray fluorescence spectroscopy (XRF) and some trace elements by ICP-MS on LDG, associated sandstones and one sand sample (Table 1). The mean SiO_2 value for our LDG samples is 96.9 ± 2.4 wt% ($n = 7$) and the darkish green samples are more enriched in Al_2O_3, Fe_2O_3, TiO_2, MgO, Cr, and Ni compared with the light yellow, more translucent samples. Loss on ignition and CO_2 were not determined. The deficiencies in the total sum are approximately proportional to secondary carbonate contents in the sandstones. In a Zr *vs.* TiO_2 diagram (Fig. 2), the sandstone samples from the LDG area plot within the field of LDG samples from this work and from Barrat *et al.* (1997), whereas the sandstones from BP and Oasis craters in Libya (Abate *et al.*, 1999) are generally more depleted in Zr and most do not plot in the LDG field. Surface sand samples from the LDG area have variable Zr and TiO_2 concentrations and define a broad field within the sandstones, including LDG data.

Figure 3 shows two diagrams with Rb, Sr (Fig. 3a), Sm and Nd (Fig. 3b) concentrations of LDG and sandstone samples from different areas. In both plots, considerable conformity exists between the LDG samples and the sandstones from the LDG strewn field and from Oasis and BP craters in Libya (additional data from Barrat *et al.*, 1997 and Abate *et al.*, 1999).

The diagrams point to geochemical relationships between the sandstones and LDG in general, but closer insights cannot be obtained on basis of such chemical data alone.

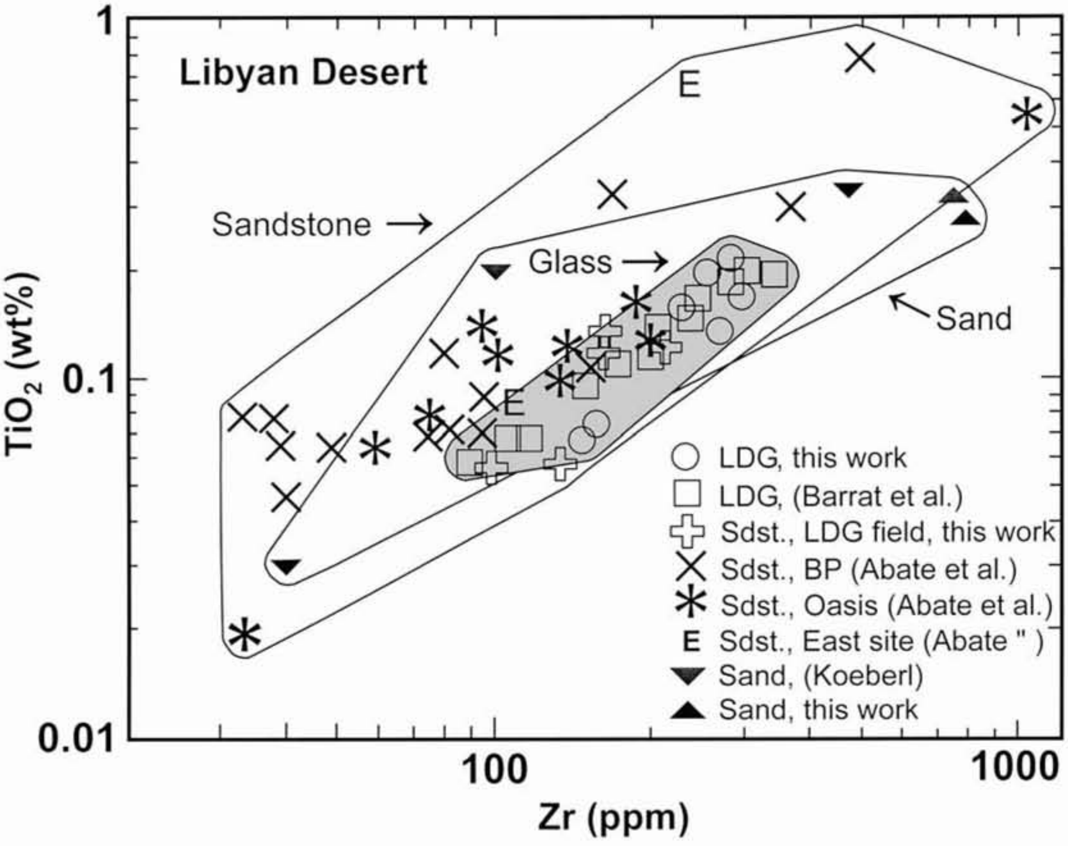

FIG. 2. Zr (ppm) *vs.* TiO_2 (wt%) diagram for LDG, sandstone and surface sand samples from the Libyan Desert. Data are from this work (Table 1) and from literature: Barrat *et al.* (1997, LDG samples); Abate *et al.* (1999, BP and Oasis craters and east of these craters (E)); Koeberl (1997, surface sand). LDG samples define a compact (shaded) field within the surface sand and sandstone sample fields, including 12 sandstone samples. Twenty other sandstone samples and all surface sand samples plot outside the LDG field.

TABLE 1. Major element and some trace element concentrations of a sand sample, five sandstones and seven LDG samples from the LDG strewn field.*

	Sand		Sandstones					LDG						
Sample	Sd C1	Sd C1(II)	S 1 ~15% $CaCO_3$	S 2 ~9% $CaCO_3$	S 3 ~6.5% $CaCO_3$	S 4 ~1.5% $CaCO_3$	S 5 ~8.5% $CaCO_3$	1 Kl inter-mediate	2 Kl dark green	3 Kl light yellow	4 Kl inter-mediate	5 Kl dark green with layers	6 Po light yellow	7 Po dark green
XRF (wt%)														
SiO_2	82.11	85.21	86.60	93.31	91.12	96.82	84.38	98.13	96.95	100.16	98.55	95.02	92.99	96.74
TiO_2	0.33	0.29	0.13	0.06	0.06	0.12	0.12	0.13	0.21	0.07	0.16	0.17	0.08	0.22
Al_2O_3	2.55	1.76	1.47	1.04	0.49	0.95	1.40	0.84	2.27	0.65	1.49	1.07	0.83	2.15
Fe_2O_3 tot	0.64	0.48	0.21	0.21	0.06	0.10	0.12	0.11	0.47	0.09	0.19	0.16	0.08	0.41
MnO	0.01	0.01	0.01	0.03	<0.01	<0.01	<0.01	<0.01	<0.01	<0.01	<0.01	<0.01	<0.01	<0.01
MgO	0.16	0.10	0.24	0.15	0.02	0.07	0.11	<0.001	0.01	0.01	0.01	0.02	<0.001	0.01
CaO	0.34	0.23	3.33	2.16	0.63	1.62	2.69	<0.001	<0.001	<0.001	<0.001	<0.001	<0.001	<0.001
Na_2O	<0.001	0.06	<0.001	<0.001	<0.001	<0.001	<0.001	<0.001	<0.001	<0.001	<0.001	<0.001	<0.001	<0.001
K_2O	0.34	0.31	0.06	0.03	0.01	0.03	0.04	0.01	0.04	<0.01	0.01	0.02	0.01	0.03
P_2O_5	0.02	0.02	0.04	0.09	0.03	0.06	0.06	0.01	0.02	0.02	0.02	0.02	0.01	0.02
L.O.I.	n.d.	n.d.	n.d.	n.d.	n.d.	n.d.	n.d.	n.d.	n.d.	n.d.	n.d.	n.d.	n.d.	n.d.
Total	86.50	88.47	92.09	97.08	92.42	99.77	88.92	99.23	99.97	101.00	100.43	96.48	94.00	99.58
XRF (ppm)														
Ba	90	77	299	97	46	44	291	8	36	9	23	27	15	22
Zr	745	788	162	97	138	200	162	258	257	149	228	288	153	282
ICP-MS (ppm)														
Cr	5.9	n.d.	14.2	20.1	17.7	13.8	5.3	n.d.	39.5	n.d.	n.d.	n.d.	35.3	n.d.
Co	1.0	n.d.	0.4	3.4	0.2	0.2	0.5	n.d.	0.3	n.d.	n.d.	n.d.	0.2	n.d.
Ni	2.3	n.d.	1.7	5.1	0.9	1.1	1.2	n.d.	4.4	n.d.	n.d.	n.d.	2.5	n.d.
Cu	1.1	n.d.	2.2	3.8	0.7	1.5	2.3	n.d.	0.5	n.d.	n.d.	n.d.	1.1	n.d.
Zn	6.1	n.d.	3.7	4.5	1.9	1.9	5.8	n.d.	3.1	n.d.	n.d.	n.d.	1.7	n.d.
W	2.6	n.d.	3.6	4.1	5.1	4.0	3.2	n.d.	8.7	n.d.	n.d.	n.d.	8.9	n.d.
Au (ppb)	<0.2	n.d.	3.6	<0.2	<0.2	<0.2	1.5	n.d.	0.7	n.d.	n.d.	n.d.	0.7	n.d.
Pb	0.90	n.d.	0.45	0.68	0.32	0.33	1.19	n.d.	0.17	n.d.	n.d.	n.d.	0.05	n.d.
Bi	0.05	n.d.	0.06	0.07	0.06	0.04	0.11	n.d.	0.04	n.d.	n.d.	n.d.	0.07	n.d.

*Sample Sd C1 (II): analysis of a second aliquot. n.d. = not determined; < = below detection limit. LDG samples labeled "Kl" were collected by B. Kleinmann, samples labeled "Po" by E. and K. Pongratz. LDG sample locations are nearly identical to the coordinates given for the sandstones in the text. $CaCO_3$ contents were calculated from microscopic analyses (point counting). XRF analyses on bulk LDG samples were carried out at Munich University, using a Philips PW 1480 wavelength-dispersive XRF-spectrometer. Standards: G-2 (granite) and quartz (laboratory-internal standard). ICP-MS analyses were performed by Actlabs, Canada (Agua regia digestion). Standards: GXR-1 (jasperoid), GXR-2 (soil), GXR-4 (porphyry copper mill heads) and GXR-6 (soil).

RUBIDIUM-STRONTIUM AND SAMARIUM-NEODYMIUM ISOTOPIC DATA: ANALYTICAL PROCEDURES AND RESULTS

From the seven LDG pieces, chunks of 2–5 g were cut with a diamond saw, and superficial alterations were removed mechanically. Pieces were cleaned in suprapure acetone, crushed in a stainless steel mortar and passed through plastic sieves to obtain 60–100 μm grain size fractions.

Two to three gram sandstone pieces were cleaned in acetone, crushed with a steel hammer and milled down in an agate mortar to grain sizes of ~60 μm.

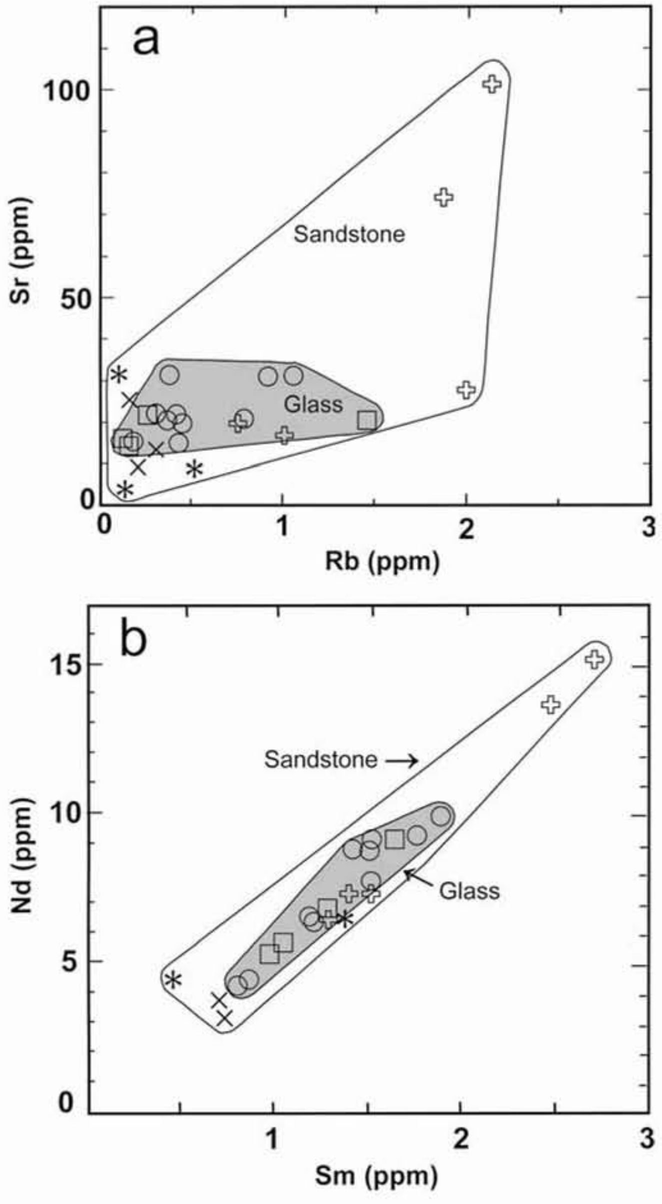

FIG. 3. (a) Rb *vs.* Sr (ppm) and (b) Sm *vs.* Nd (ppm) concentration diagrams for LDG samples (shaded) and sandstone samples from the LDG strewn field and from the Libyan craters. For symbols see Fig. 2.

Aliquots of 60–150 mg sample powders were brought into solution with hydrofluoric acid, perchloric acid, and hydrochloric acid. In two different sets of ion exchange columns ultrapure Rb, Sr, Sm and Nd fractions were obtained. Elemental concentrations *via* the isotope dilution technique and isotopic compositions were determined at the Munich laboratory with a multicollector Finnigan MAT 261 thermal ionisation mass spectrometer under static conditions for Sr and Sm and under dynamic conditions for Nd. Rb concentrations were determined with a Finnigan thermal ionisation quadrupole mass spectrometer (THQ). Total procedural blanks during the run of these samples were 1 ng Sr and 100 pg Nd ($n = 4$).

Table 2 reports the isotopic results together with analytical data from three LDG aliquots already published by Horn *et al.* (1997). Sr concentrations of LDG are relatively uniform between 15 and 32 ppm. The sandstone samples show more heterogeneous values from 17 to 103 ppm, which are approximately proportional to the different amounts of carbonate in the samples. The influence of carbonate in these sandstones also shows up in the less radiogenic ^{87}Sr/^{86}Sr ratios of 0.7091 to 0.7105. The ^{87}Sr/^{86}Sr ratios of LDGs between 0.7122 and 0.7134 are distinct from those of the sandstones, with a trend showing the darkish green samples to be more radiogenic than the transparent yellow specimens.

Concerning the Sm-Nd isotopic system, 10 LDG samples have very homogeneous ϵ-Nd values between –17.8 and –16.1 and Nd model ages from 1.42 to 1.61 Ga and 1.81 to 2.00 Ga for chondritic uniform reservoir (CHUR) and depleted mantle reservoir (Liew and Hofmann, 1988) models, respectively. The sandstones show significantly higher ϵ-Nd values from –9.6 to –6.9 and lower Nd model ages between 0.66 to 1.02 Ga (CHUR) and 1.26 to 1.63 Ga (depleted mantle reservoir) than the LDG samples.

Isotopic data on LDG by Barrat *et al.* (1997; four samples, the Sr isotopic data were adjusted to ^{87}Sr/^{86}Sr = 0.710248 for NBS 987 to compare them with our data) are included in two isotopic evolution diagrams. For the 14 LDG samples a Rb-Sr regression line indicates an age of 557 ± 132 Ma (1σ) (Fig. 4). The initial ^{87}Sr/^{86}Sr value is 0.71209 ± 0.00015 (1σ). A nearly identical age of 523 ± 126 Ma (initial ^{143}Nd/^{144}Nd ratio: 0.51138 ± 0.00009) is obtained when considering the Sm-Nd isotopic system (Fig. 5).

The five sandstone samples from the LDG strewn field do not show a comparable correlation either in the Rb-Sr or the Sm-Nd isotopic system.

The regression lines were calculated using the method of least squares without taking into account the individual errors (see handbooks of error calculation, *e.g.*, Hänsel, 1965). Consequently the errors in age and initial isotopic ratios are defined by the scatter of the points alone. This procedure avoids influences in the results by different weighting factors.

When a chi-square test is applied to the regression, some assumptions about the reproducibility of the measurements of the isotope ratios must be made, because we know little about the reproducibility of the measurements of such glass samples.

TABLE 2. Rb-Sr and Sm-Nd elemental concentrations, isotope ratios and Nd model ages for LDG and sandstone samples from the LDG strewn field.*

Sample	Rb (ppm)	Sr (ppm)	$^{87}Rb/^{86}Sr$	$^{87}Sr/^{86}Sr \pm 2\sigma_M$	Sm (ppm)	Nd (ppm)	$^{147}Sm/^{144}Nd$	$^{143}Nd/^{144}Nd \pm 2\sigma_M$	ϵ-Nd	t_{CHUR} (Ma)	t_{DM} (Ma)
LDG											
1Cl-A†	0.40	21.5	0.053	0.712588 10	1.51	9.18	0.0998	0.511727 07	−17.8	1431	1816
1Cl-B†	0.37	20.9	0.051	0.712602 14	1.45	8.78	0.0997	0.511727 06	−17.8	1429	1814
1Cl-C†	0.81	21.0	0.112	0.712513 14	1.45	8.81	0.0996	0.511733 08	−17.7	1419	1805
1Kl	0.31	22.2	0.040	0.712342 11	1.20	6.43	0.1124	0.511756 12	−17.2	1591	1988
2Kl	1.05	31.1	0.097	0.713439 10	1.86	9.93	0.1131	0.511764 09	−17.0	1588	1990
3Kl	0.17	15.0	0.033	0.712389 11	0.86	4.65	0.1115	0.511762 21	−17.1	1564	1963
4Kl	0.38	31.8	0.035	0.712521 13	1.51	7.81	0.1171	0.511812 12	−16.1	1579	1996
5Kl	0.45	20.0	0.066	0.712194 15	1.18	6.56	0.1089	0.511751 10	−17.3	1537	1932
6Po	0.43	15.2	0.082	0.712658 09	0.80	4.33	0.1115	0.511787 13	−16.6	1520	1928
7Po	0.91	31.3	0.085	0.713331 09	1.74	9.26	0.1138	0.511763 09	−17.1	1605	2004
Sandstone											
S1	2.13	103.0	0.060	0.709098 11	2.68	15.31	0.1060	0.512147 10	−9.6	826	1353
S2	1.99	28.3	0.204	0.709278 10	1.28	6.61	0.1175	0.512206 12	−8.4	832	1427
S3	0.76	20.1	0.109	0.709647 08	1.51	7.14	0.1279	0.512177 10	−9.0	1023	1626
S4	0.98	17.0	0.166	0.710527 14	1.38	7.33	0.1140	0.512282 11	−6.9	657	1260
S5	1.86	73.9	0.073	0.709500 09	2.45	13.65	0.1084	0.512157 16	−9.4	831	1368

*Errors of the isotope ratios refer to the last digits, M (mean) of ~60 individual ratios. Error for $^{87}Rb/^{86}Sr$: $1\sigma = 2\%$ and for $^{147}Sm/^{144}Nd$: $1\sigma = 0.4\%$. $^{87}Sr/^{86}Sr$ values are adjusted to 0.710248 for NBS 987 and normalised to $^{86}Sr/^{88}Sr = 0.1194$. $^{143}Nd/^{144}Nd$ values were normalised to $^{146}Nd/^{144}Nd = 0.7219$. Measurements of NBS 987 amount to $^{87}Sr/^{86}Sr = 0.710251 \pm 19$ (1σ), $n = 24$, during analyses of 1C1-A, -B, and -C samples, and $^{87}Sr/^{86}Sr = 0.710274 \pm 33$ (1σ), $n = 17$, concerning all other samples. Present-day values for CHUR are: $^{143}Nd/^{144}Nd = 0.512638$ and $^{147}Sm/^{144}Nd = 0.1967$. Depleted mantle (DM) values are: $^{143}Nd/^{144}Nd = 0.513151$ and $^{147}Sm/^{144}Nd = 0.219$ (Liew and Hofmann,1988). Decay constants used: $\lambda^{87}Rb = 1.42 \times 10^{-11}$ year^{-1} and $\lambda^{147}Sm = 6.54 \times 10^{-12}$ year^{-1}.

†Already published in Horn *et al.* (1997).

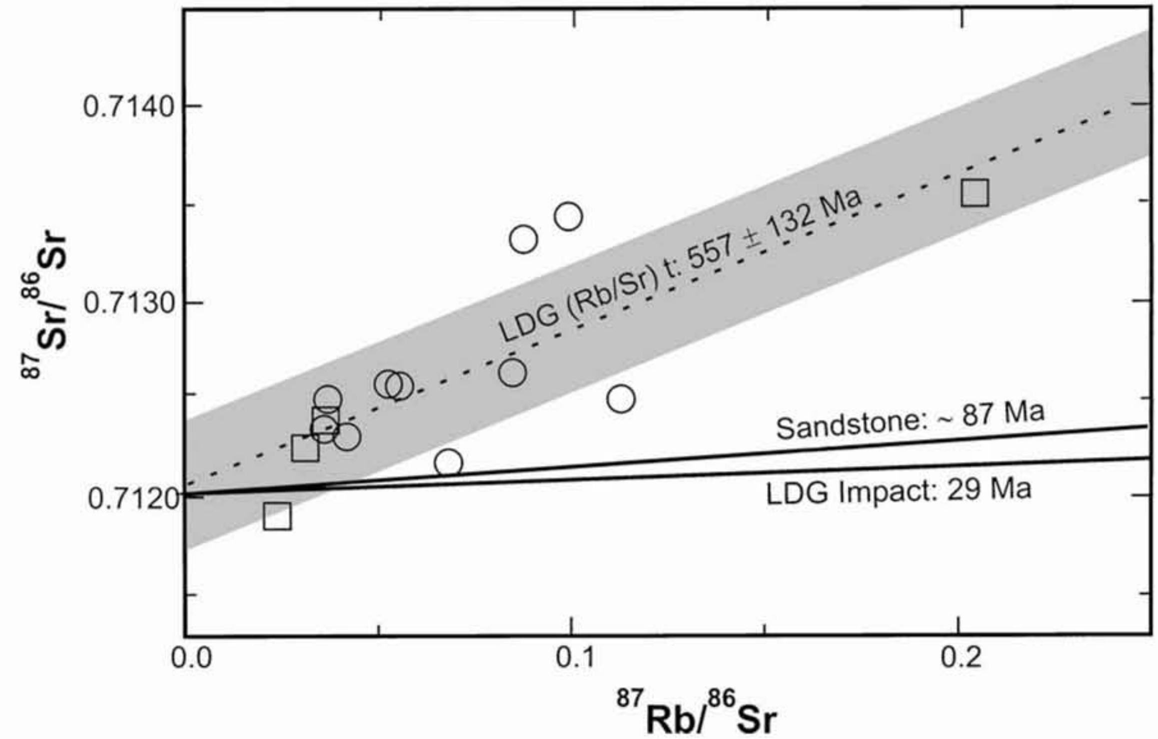

FIG. 4. Rb-Sr isotopic evolution diagram for 14 LDG samples. A linear regression through all sample points yields an age of 557 ± 132 Ma with an initial $^{87}Sr/^{86}Sr$ ratio of 0.71209 ± 0.00015. Shaded area corresponds to the deviation ($\pm 1\sigma$) of the $^{87}Sr/^{86}Sr$ values. Reproducibility error bars for the samples are smaller than the symbols. Reference lines corresponding to 29 Ma (impact event) and to ~87 Ma (stratigraphic age of the Saad Sandstone Formation) are also plotted. For symbols see Fig. 2.

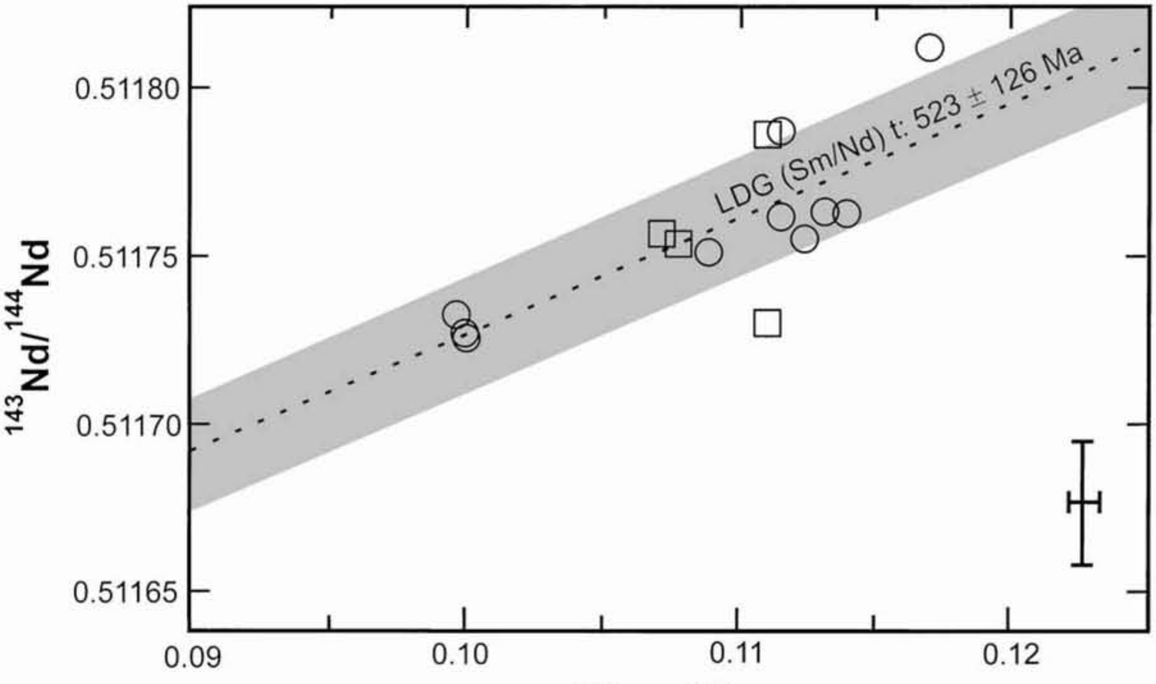

FIG. 5. Sm-Nd isotopic evolution diagram for the same 14 LDG samples as in Fig. 4. The age obtained from the inclination of the regression line is 523 ± 126 Ma with an initial $^{143}Nd/^{144}Nd$ ratio of 0.51138 ± 0.00009. Reproducibility, shown as error cross, for the $^{143}Nd/^{144}Nd$ values is ±35 ppm and ±0.4% for $^{147}Sm/^{144}Nd$. Shaded area is defined in Fig. 4. For symbols see Fig. 2.

A realistic approximation for the analytical errors of the isotopic ratios of the glass samples may be similar to the reproducibility of measurements of pure isotopic standard material (±45 ppm for $^{87}Sr/^{86}Sr$ and ±35 ppm for $^{143}Nd/^{144}Nd$). If so, the mean square weighted deviation (MSWD) is 86 for the Rb/Sr system and 0.85 for the Sm/Nd system.

DISCUSSION

Rubidium-Strontium and Samarium-Neodymium Geochronology

It has been shown by various authors on tektite strewn fields worldwide that Rb-Sr and Sm-Nd isotopic analyses of tektites can be used to determine the age and provenance of the target materials that were impact melted to form these objects (*e.g.* Schnetzler and Pinson, 1964; Shaw and Wasserburg, 1982; Blum *et al.*, 1992; Premo and Izett, 1992). In the case of the Australasian impact event, which has been dated at 0.7 Ma (Zähringer, 1963), it could be shown that the Muong Nong-type tektites yield a Rb-Sr isochron age of 167 ± 12 Ma, corresponding to the deposition time of the sedimentary target material (Blum *et al.*, 1992).

While the formation of LDG undoubtedly happened at ~29 Ma (fission-track results from Bigazzi and de Michele, 1997 and Horn *et al.*, 1997), we cannot recognise a homogenisation of the Rb-Sr system in the glass during this event. The high Rb-Sr age of 560 ± 130 Ma obtained in this study gives first evidence for this and is confirmed by the Sm-Nd age of 520 ± 130 Ma. Both age determinations are not very precise. The 1σ error is ~25%, which undoubtedly causes some limitations for any geochronological interpretation. In the case of the Sm-Nd system the data would form a linear array by taking individual weights into account (MSWD < 1) but the small data spread of x-values causes the high error. In the isotopic evolution diagram of the Rb-Sr system the scatter of points is dominant and a calculation of the MSWD yields a very high value. Although the disturbance of this system is significant, Rb volatilisation and/or Rb-Sr fractionation effects upon melting or other processes in the time between approximately 540 and 29 Ma were not sufficient to eliminate the information about the Pan-African age of the precursor (Fig. 4).

The sandstones from the "Nubian Group", generally considered to be the LDG target material, are stratigraphically classified by Klitzsch (1978) as late Cretaceous, probably Coniacian (~87 Ma) and therefore considerably younger than indicated by our LDG isotope data. On the other hand, a compilation of literature data for granitoid rocks in northeast Africa west of the Nile shows that 13 Rb-Sr whole-rock intrusion ages define a mean value of 598 ± 71 Ma which belongs undoubtedly to the Pan-African orogeny (Fig. 6) and corresponds well to the mean value of 540 ± 90 Ma shown

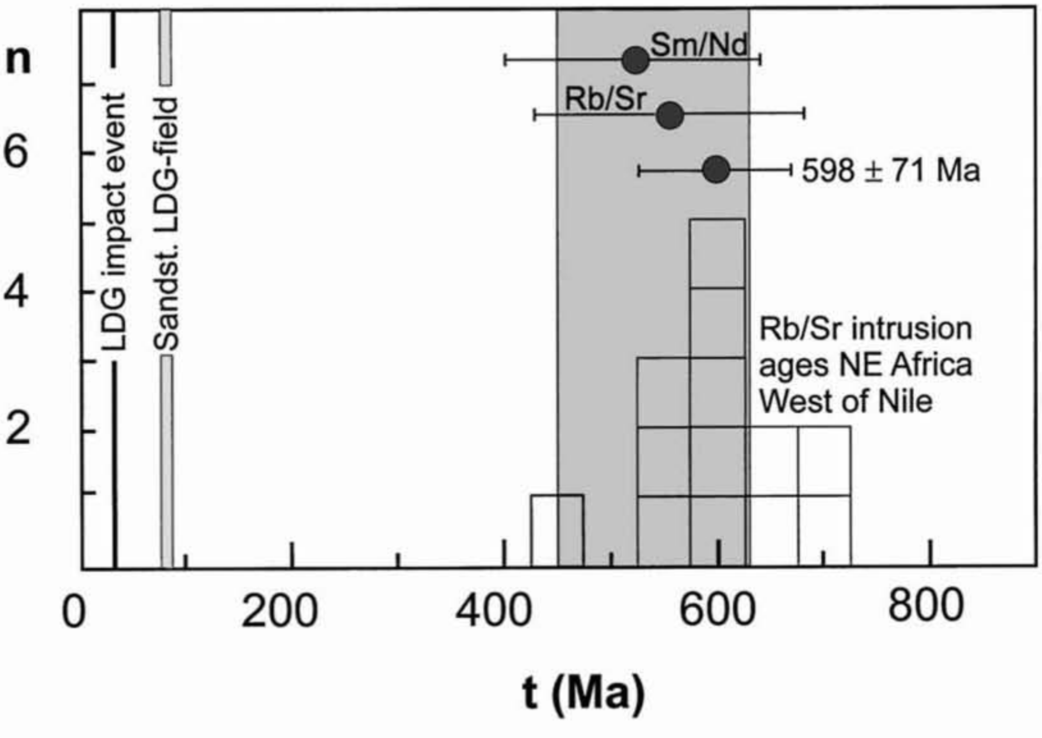

FIG. 6. Histogram of 13 Rb-Sr whole-rock intrusion ages for granitoid rocks from northeast Africa west of the Nile, defining a mean value of 598 ± 71 Ma. This value is in good agreement with the mean value of 540 ± 90 Ma (shaded area) from the two regression analyses. For comparison, the impact event and the stratigraphic age of the LDG field sandstones are marked. Data for the granitoid rocks are from Pegram *et al.* (1976), Schandelmeier and Darbyshire (1984), and Harms *et al.* (1990).

shaded in Fig. 6. These age values are in fairly good concordance which gives strong evidence for LDG target material of Pan-African age, whatever it was petrographically.

In the case of the sandstones it can be argued that the LDG sandstones and those from the Libyan craters could have had originally also Pan-African age signatures but were lost during sedimentation, mixing or alteration processes. However, we consider the different carbonate contents in the sandstones as originating from the standstones themselves. Seawater alteration of the late Cretaceous "Nubian Sandstones" (Klitzsch, 1978) was not the most probable scenario as the last marine transgression in the Great Sand Sea occurred earlier during the Albian-Aptian (97–124.5 Ma; Reynolds *et al.*, 1997).

The Correlation: Epsilon-Neodymium *versus* Strontium-87/Strontium-86

^{87}Sr/^{86}Sr ratios and ϵ-Nd values for LDG and sandstone samples from Table 2 reveal some incompatibility of these data. In Fig. 7, an ϵ-Nd *vs.* ^{87}Sr/^{86}Sr diagram with the measured isotopic ratios, the LDG samples plot in a narrow range and are distinct from the sandstone samples from the LDG strewn field. Data from BP and Oasis crater sandstones, published by Abate *et al.* (1999), are included for comparison. Their sample BP-U-16-1 was plotted erroneously and its ϵ-Nd parameter was recalculated by us from their isotopic ratios which makes a genetic relationship between LDG and the Oasis and BP sandstones less probable than suggested by those authors.

Figure 7 includes the field for Precambrian granitic rocks of northeast Africa which overlaps the LDG completely and BP and Oasis crater sandstones at least partly. In contrast, data for sandstones from the LDG strewn field plot outside the granitoid area. From Fig. 7 it can also be inferred that a possible mixing of Precambrian granitic rocks and Mesozoic sandstones is not a very likely model to form the composite LDG target material.

Neodymium Model Ages

Finally, we present a comparative histogram with Nd model ages for LDG, sandstone and granitoid rocks (Fig. 8). Model ages for LDG, calculated relative to CHUR, are concentrated

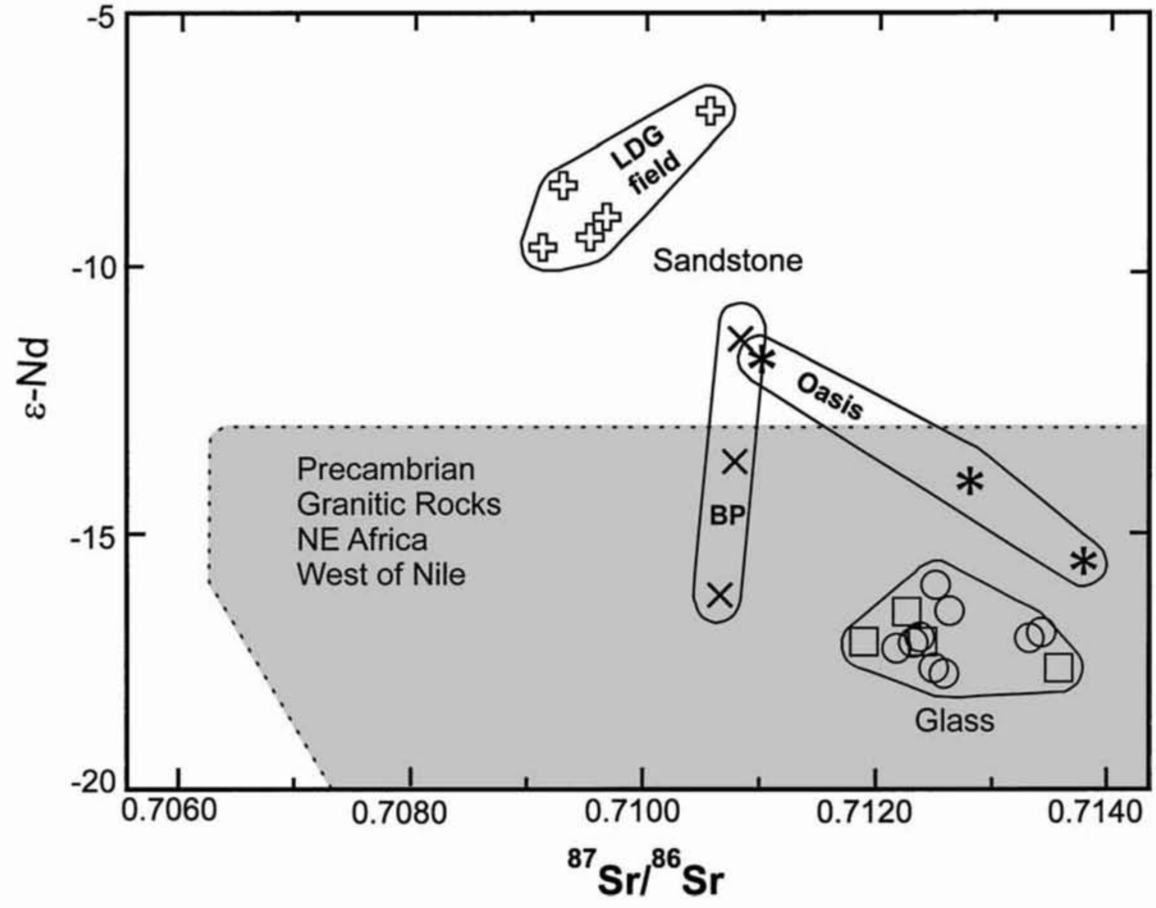

FIG. 7. Present-day ϵ-Nd *vs.* ^{87}Sr/^{86}Sr ratios of 14 LDG samples, three sandstone samples from BP and Oasis craters, Libya, and five sandstone samples from the LDG strewn field (for symbols see Fig. 2). Data for Precambrian granitic rocks from northeast Africa west of the Nile (shaded area) are from the same references as in Fig. 6.

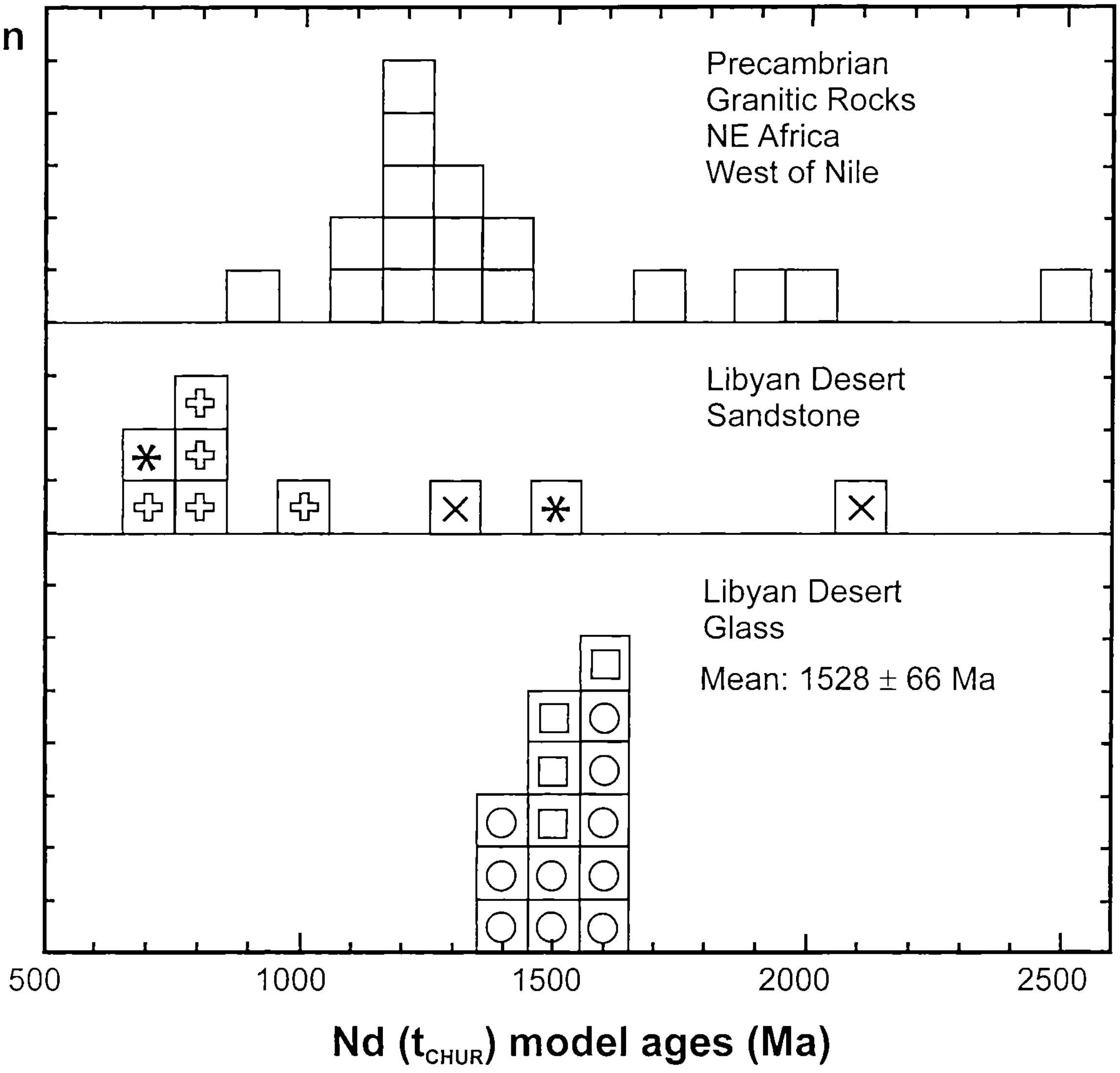

FIG. 8. Nd (t_{CHUR}) model age histogram for 14 LDG samples (bottom), Libyan Desert sandstones from the LDG strewn field and BP and Oasis craters (middle) and Precambrian granitic rocks (top). For symbols see Fig. 2, data sources for granitic rocks see Fig. 6.

between 1.42 and 1.61 Ga, and form a distribution with a mean value of 1528 ± 66 Ma. This implies that the parent material in the targets rocks was most likely derived from Precambrian crustal material. The sandstone samples from the LDG area have considerably lower Nd model ages between 0.66 and 1.02 Ga whereas the granitoid rocks cover a wide range from 0.9 Ga to 2.5 Ga with a maximum at 1.2 Ga, closer to the LDG values than those from the sandstones. We have also calculated Nd model ages from the analytical data given by Abate *et al.* (1999) for the Libyan crater sandstones. Two samples from the BP structure and two samples from Oasis crater have highly heterogeneous model ages between 0.67 and 2.04 Ga, not consistent with LDG data. If we use parameters for the depleted mantle reservoir in our calculation, data for all samples were shifted towards higher Nd model ages but the differences between them does not change.

CONCLUSIONS

Libyan Desert Glass Sr and Nd isotopic signatures are more comparable to Pan-African granitic rocks of northeast Africa west of the Nile than to those from quartz-rich sandstones of the LDG strewn field and adjacent areas. This can be deduced from the combination of Rb-Sr and Sm-Nd geochronological data, Sr and Nd isotopic ratios and Nd model ages. Our new isotopic data almost certainly exclude the Libyan BP and Oasis craters as source impact structures for the LDG. We do not necessarily and exclusively have to look for LDG-related impact crater structures, as nobody has yet seen and described the effects of cometary impacts, the preferred scenario for LDG formation by Seebaugh and Strauss (1984), which also been proposed by Horn *et al.* (1997).

The observation of PDFs in some sandstone samples from the LDG area in the Great Sand Sea by Kleinmann *et al.* (2001) proves that parts of this material were affected by a shock event, but the isotopic evidence proves, too, that these or similar rocks cannot properly be regarded as possible source materials for LDG.

We still do not have profound knowledge of the palaeographic situation of the Great Sand Sea during the formation of LDG, some 30 Ma ago. It is clear, however, that the material from recent dunes is not identical to Oligocene sand in that region. The results of our work best characterise the target material of LDG as sand derived from an old, Precambrian Pan-African crystalline basement. However, it should be investigated in more detail what processes happen when a meteorite impacts directly crystalline (granitoid) rocks.

Acknowledgements–Because the scientific work of this paper was not supported by any grants, the authors are indebted to B. Kleinmann and E. and K. Pongratz who generously provided LDG, sand and sandstone samples from the Great Sand Sea, Egypt, and to T. Dorfner and J. Robles for XRF analyses and Rb measurements. Many thanks to P. Horn and J. Pohl for their suggestions on an earlier version of the manuscript, to Alison Dalfovo and Bill Bandy for correcting our English and to Gabriel Valdez for the drawing of the figures. Reviews by Christian Koeberl, an anonymous reviewer and editoral comments by Kevin McKeegan helped to clarify the original manuscript. This paper was written during P. Schaaf's sabbatical stay at the Institut für Mineralogie, Petrologie und Geochemie, Universität München.

Editorial handling: K. D. McKeegan

REFERENCES

ABATE B., KOEBERL C., KRUGER J. F. AND UNDERWOOD J. R., JR. (1999) BP and Oasis impact structures, Libya, and their relation to Libyan Desert Glass. In *Large Meteorite Impacts and Planetary Evolution II* (eds. B. O. Dressler and V. L. Sharpton), pp. 177–192. Geol. Soc. Am. Spec. Paper **339**, Boulder, Colorado, USA.

BARRAT J. A., JAHN B. M., AMOSSÉ J., ROCCHIA R., KELLER F., POUPEAU G. R. AND DIEMER E. (1997) Geochemistry and origin of Libyan Desert glasses. *Geochim. Cosmochim. Acta* **61**, 1953–1959.

BIGAZZI G. AND DE MICHELE V. (1997) New fission-track ages of Libyan Desert Glass. In *Proceedings, Silica '96, Meeting on Libyan Desert Glass and Related Events* (ed. V. de Michele), pp. 49–57. Sahara, Pyramids, Milano, Italy.

BLUM J., PAPANASTASSIOU D. A., KOEBERL C. AND WASSERBURG G. J. (1992) Neodymium and strontium isotopic study of Australasian tektites: New constraints on the provenance and age of target materials. *Geochim. Cosmochim. Acta* **56**, 483–492.

DE MICHELE V., ED. (1997) *Proc. "Silica '96", Meeting on Libyan Desert Glass and Related Events.* Pyramids, Segrate (Milano), Italy. 158 pp.

DIEMER E. (1997) Libyan Desert Glass: An impactite. State of the art in July 1996. In *Proceedings, Silica '96, Meeting on Libyan Desert Glass and Related Events* (ed. V. de Michele), pp. 95–105. Sahara, Pyramids, Milano, Italy.

GENTNER W., STORZER D. AND WAGNER G. A. (1969) New fission track ages of tektites and related glasses. *Geochim. Cosmochim. Acta* **33**, 1075–1081.

HÄNSEL H. (1965) *Grundzüge der Fehlerrechnung.* VEB Deutscher Verlag der Wissenschaften, Berlin, Germany. 115 pp.

HARMS U., SCHANDELMEIER H. AND DARBYSHIRE D. P. F. (1990) Pan-African reworked early/middle Proterozoic crust in NE Africa west of the Nile: Sr and Nd isotope evidence. *J. Geol. Soc. London* **147**, 859–872.

HERMINA M., KLITZSCH E. AND LIST F. K. (1989) *Stratigraphic Lexicon and Explanatory to the Geological Map of Egypt 1:500,000.* Conoco Inc., Cairo, Egypt. 263 pp.

HORN P., MÜLLER-SOHNIUS D., SCHAAF P., KLEINMANN B. AND STORZER D. (1997) Potassium-argon and fission-track dating of Libyan Desert Glass, and strontium- and neodymium isotope constraints on its source rocks. In *Proc. "Silica '96", Meeting on Libyan Desert Glass and Related Events* (ed. V. de Michele), pp. 59–73. Pyramids, Segrate (Milano), Italy.

KLEINMANN B. (1969) The breakdown of zircon observed in the Libyan Desert Glass as evidence of its impact origin. *Earth Planet. Sci. Lett.* **5**, 497–501.

KLEINMANN B., HORN P. AND LANGENHORST F. (2001) Evidence for shock metamorphism in sandstones from the Libyan Desert Glass strewn field. *Meteorit. Planet. Sci.* **36**, 1277–1282.

KLITZSCH E. (1978) Geologische Bearbeitung Südwest-Ägyptens. *Geologische Rundschau* **67**, 509–520.

KOEBERL C. (1997) Libyan Desert Glass: Geochemical composition and origin. In *Proc. "Silica '96", Meeting on Libyan Desert Glass and Related Events* (ed. V. de Michele), pp. 121–131. Pyramids, Segrate (Milano), Italy.

KOEBERL C. (2000) Confirmation of a meteoritic component in Libyan Desert Glass from osmium-isotopic data (abstract). *Meteorit. Planet. Sci.* **35 (Suppl.)**, A89–A90.

LIEW T. C. AND HOFMANN A. (1988) Precambrian crustal components, plutonic associations, plate environment of the Hercynian Fold Belt of central Europe: Indications from a Nd and Sr isotopic study. *Contrib. Mineral. Petrol.* **98**, 129–138.

MÜLLER-SOHNIUS D., HORN P., PREUSS E. AND STORZER D. (1993) Neue Spaltspuren- und K-Ar-Alter von Libyschem Wüstenglas (abstract). *Europ. J. Mineral.* **5**, 138.

MURALI A. V., ZOLENSKY M. E., UNDERWOOD J. R., JR. AND GIEGENGACK R. (1997) Chondritic debris in Libyan Desert Glass. In *Proc. "Silica '96", Meeting on Libyan Desert Glass and Related Events* (ed. V. de Michele), pp. 133–142. Pyramids, Segrate (Milano), Italy.

PEGRAM W. J., REGISTER J. K., JR., FULLAGAR P. D., GHUMA M. A. AND ROGERS J. J. W. (1976) Pan-African ages from a Tibesti massif batholith, southern Libya. *Earth Planet. Sci. Lett.* **30**, 123–128.

PREMO W. R. AND IZETT G. A. (1992) Isotopic signatures of black tektites from the K-T boundary on Haiti: Implications for the age and type of source material. *Meteoritics* **27**, 413–423.

REYNOLDS P-O., SCHANDELMEIER H. AND SEMPTER A. K. (1997) The early Cretaceous (Aptian, ca 115 Ma). In *Palaeogeographic-Palaeotectonic Atlas of North-Eastern Africa, Arabia, and Adjacent Areas. Late Neoproterozoic to Holocene* (eds. H. Schandelmeier and P-O. Reynolds), pp. 73–79. A. A. Balkema, Rotterdam, The Netherlands.

ROCCHIA R., ROBIN E., FRÖHLICH F., AMOSSÉ J., BARRAT J. A., MÉON H., FROGET L. AND DIEMER E. (1997) The impact origin of Libyan Desert Glass. In *Proc. "Silica '96", Meeting on Libyan Desert Glass and Related Events* (ed. V. de Michele), pp. 143–149. Pyramids, Segrate (Milano), Italy.

SCHANDELMEIER H. AND DARBYSHIRE D. P. F. (1984) Metamorphic and magmatic events in the Uweinat-Bir Safsaf uplift (Western Desert, Egypt). *Geologische Rundschau* **73**, 819–831.

SCHNETZLER C. C. AND PINSON W. H. (1964) Variation of strontium isotopes in tektites. *Geochim. Cosmochim. Acta* **28**, 953–969.

SEEBAUGH W. R. AND STRAUSS A. M. (1984) A cometary impact model for the source material of Libyan Desert Glass. *J. Non-Crystalline Solids* **67**, 511–519

SHAW H. F. AND WASSERBURG G. J. (1982) Age and provenance of the target materials for tektites and possible impactites as inferred from Sm-Nd and Rb-Sr systematics. *Earth Planet. Sci. Lett.* **60**, 155–177.

STORZER D. AND KOEBERL C. (1991) Uranium and zirconium enrichments in Libyan Desert Glass. Zircon, baddeleyite and high temperature history of the glass (abstract). *Lunar Planet. Science* **22**, 1345–1346.

WEEKS R. A., UNDERWOOD J. R., JR. AND GIEGENGACK R. (1984) Libyan Desert Glass: A review. *J. Non-Crystalline Solids* **67**, 593–619.

ZÄHRINGER J. (1963) K-Ar measurements of tektites. In *Radioactive Dating*, pp. 289–305. Intern. Atomic Energy Agency, Vienna, Austria.